

HYPERCHARGE EXCHANGE REACTIONS AND HYPERON RESONANCE PRODUCTION

A.C. Irving

Department of Applied Mathematics and Theoretical Physics, Liverpool University, Liverpool L69 3BX, U.K.

ABSTRACT

A review is presented of recent high statistics results on hypercharge exchange processes. Intermediate energy data on helicity non-flip dominated processes (Σ production) and on helicity-flip processes (Σ^* production) reveal complicated and strongly energy-dependent systematics for exchange degeneracy breaking. Preliminary data at 70 GeV/c show evidence of the expected effects of high-lying J-plane singularities at $|t|_{\lambda} > 0.5$. No existing model, or simple modification thereof, can describe the major features of the new data.

1. INTRODUCTION

In this short report I shall discuss what lessons may be learned from the recent experimental results on hypercharge exchange (HYCEX) processes. The latter represent one of the final attempts to achieve a simple understanding of two-body hadronic exchange mechanisms. Since the instigation of these experiments to measure

$$K^- p \rightarrow \pi^- \Sigma^+ \quad (1a)$$

$$\pi^+ p \rightarrow K^+ \Sigma^+ \quad (1b)$$

and

$$K^- p \rightarrow \pi^- Y^*(1385)^+ \quad (2a)$$

$$\pi^+ p \rightarrow K^+ Y^*(1385)^+ \quad (2b)$$

there has been an increasing suspicion that we may, as it were, be attempting to discover QED by measuring uranium-lead scattering. Nonetheless, these HYCEX processes, together with their charge-exchange (CEX) analogues have already provided valuable information about such global, phenomenological features as Regge pole dominance, exchange-degeneracy and absorption effects. These laboriously accumulated systematics must be held in store for the day when "complete solutions" for the hadronic interaction are being tested.

Particular attractions of processes (1) and (2) are that they readily yield polarisation information, they test line-reversal symmetry (LRS) and hence EXD, they exhibit both helicity-flip and non-flip dominated cross-sections (processes (1) and (2) respectively) and they are simply related by SU(3) to CEX processes.

2. HYCEX FOLKLORE

"One may wax eloquent for many a moon on the standard folklore applied to the hypercharge exchange reactions. Here rather than a full core dump,

we present a restrained soliloquy".

G.C. Fox (Nucl. Phys. B56, 386 (1973))

The exchange amplitude structure of reactions 1a,b can be expressed as

$$K^- p \rightarrow \pi^- \Sigma^+ = V+T \equiv A_R \quad (3a)$$

$$\pi^+ p \rightarrow K^+ \Sigma^+ = -V+T \equiv A_C \quad (3b)$$

In a 2-Regge pole model ($V \equiv K^*(890)$, $T \equiv K^{**}(1420)$) these amplitudes would be

$$V = \beta_V i e^{-i\pi\alpha_V/2} s^{\alpha_V} \quad (4a)$$

$$T = \beta_T e^{-i\pi\alpha_T/2} s^{\alpha_T} \quad (4b)$$

Let us denote the differential cross-sections for processes 1a,b by σ_R , σ_C respectively ($R \equiv$ Real, $C \equiv$ Complex in a dual solution). The quantity $\tilde{\cos\phi}_{VT}$ ¹⁾, defined by

$$\tilde{\cos\phi}_{VT} \equiv (\sigma_R - \sigma_C) / (\sigma_R + \sigma_C) = 2|V/T| \cos\phi_{VT} / [1 + |V/T|^2] \quad (5)$$

gives some measure^{*} of the spin-averaged relative phase difference ϕ_{VT} between vector and tensor exchanges. In a 2-pole model (4)

$$\tilde{\cos\phi}_{VT} = 2\lambda \sin \frac{\pi}{2} (\alpha_V - \alpha_T) / [1 + \lambda^2], \quad (6)$$

where $\lambda(s,t) = (\beta_V/\beta_T) s^{\alpha_V - \alpha_T}$. Thus $\tilde{\cos\phi}_{VT}(t) \equiv 0$ if weak EXD ($\alpha_V(t) = \alpha_T(t)$) holds. It should also vanish when $\alpha_V(t) = 0$ if vector exchange has a nonsense wrong-signature zero: $\beta_V \sim \alpha_V(t)$ (cf. ρ in $\pi^- p \rightarrow \pi^0 n$). In the latter case, σ_R and σ_C would exhibit a cross-over at this t -value ($-0.4?$). Even if EXD does not hold, $\tilde{\cos\phi}_{VT}$ should vary slowly with s assuming $|\alpha_V - \alpha_T|$ is not too large (the K^* spectrum suggests less than 0.1-0.2) and that leading Regge poles do indeed dominate. Any zero structure would be independent of s .

Denoting helicity flip and non-flip amplitudes by F and N respectively, the polarisation P is given by

$$P\sigma = -2\text{Im}[NF^*] \quad (7)$$

so that

$$P_R \sigma_R + P_C \sigma_C = -2\text{Im}[N_V F_V^* + N_T F_T^*]. \quad (8)$$

* $2x/(1+x^2)$ differs from 1 by less than 20% for $0.5 < x < 2$.

In any 2-pole model this must vanish so that

$$P_R = -P_C (\sigma_R / \sigma_C). \quad (9)$$

The vector and tensor polarisation contributions to eqn. (8) are respectively analogous to those in $\pi^- p \rightarrow \pi^0 n$ and $\pi^- p \rightarrow \eta n$. If weak EXD holds, $\sigma_R = \sigma_C$ so that

$$P_R = -P_C. \quad (10)$$

If strong EXD holds ($\beta_V / \beta_T = \tan \pi \alpha / 2$, $\alpha = \alpha_V = \alpha_T$), then $F_R, N_R \sim \text{real}$ and $F_C, N_C \sim e^{-i\pi\alpha}$ so that

$$P_R = P_C = 0. \quad (11)$$

Simple coupling arguments ¹⁾ tell us that the Σ cross-sections (1) and Y^* cross-sections (2) will be helicity non-flip and flip dominated respectively. One should study both.

3. RECENT HYCEX DATA

Fig. 1 shows σ and P for reactions (1) at 7 and 10 GeV/c as measured in the experiment by Berglund et al ²⁾ at CERN. In this counter experiment and in the hybrid experiment of the SLAC/Imperial College collaboration ^{3),4)} particular attention was paid to reducing relative normalisation errors between the $K^- p$ and $\pi^+ p$ channels.

In this figure one notices: i) A cross-over in the cross-sections ($\sigma_R > \sigma_C$ at small t) which moves to smaller t as s increases. ii) A marked change in slope near $t = -0.5$ (pole/cut interference?). iii) The EXD violation drops rapidly with energy. iv) The polarization is large and approximately mirror symmetric (eqn. 10). It does not decrease with s in this range. Fig. 2 shows $\hat{\cos} \psi_{VT}$ for this data set and those of refs. 3,4.

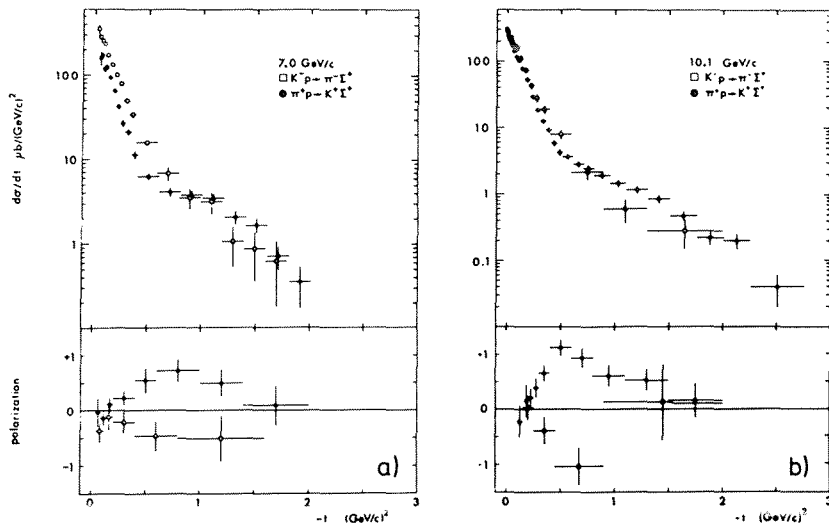


Fig. 1 HYCEX data from ref. 2.

The plots of $\tilde{\cos}\phi_{VT}$ vs. t shown in fig. 2 show many of the above features more clearly. At 7 GeV/c there may be some systematic differences at small t between the data of ref. 2 and those of ref. 4. We see:

(i) The rapid s -dependence of $\tilde{\cos}\phi_{VT}$ excludes any 2-pole model.

(ii) The Navelet and Stevens (NS) pole + low-lying effective cut model (solid curve in fig. 2a) reproduces the t dependence of $\tilde{\cos}\phi_{VT}$ well. The absorption model of Hartley and Kane (HK) with high-lying cuts does not, having too pronounced an EXD violation (dotted curve of fig. 2a). Girardi has recently applied a model with dual Regge-Pomeron, Regge-Regge and Regge-Pomeron-Regge cuts to HYCEX data. The secondary cuts do indeed give $\tilde{\cos}\phi_{VT}$ a rapid s -dependence. Since the Regge-Pomeron cuts are the traditional ones which produce $\sigma_C > \sigma_R$, one expects that, asymptotically, $\tilde{\cos}\phi_{VT} < 0$ for all t . However, already by 10 GeV/c the model predicts $\tilde{\cos}\phi_{VT}$ to be negative (-.3 at $t = -.5$) whereas the data are still positive.

(iii) The $\tilde{\cos}\phi_{VT}$ values for the Y^* processes (2) are very large. This can be partially explained by the kinematic behaviour $\sigma \sim (t_{\min} - t)$ expected in a helicity flip dominated reaction [$t_{\min}(KY^*) < 0, t_{\min}(\pi Y^*) > 0$]. The solid curves in fig. 2b give the predictions of weak EXD modified by this kinematic effect. Its major effect is at low $|t|$ and s . In the related processes $KN \rightarrow K\Delta, \bar{K}N \rightarrow \bar{K}\Delta$ where t_{\min} is much smaller, this effect is quite insufficient to explain the large values of $\tilde{\cos}\phi_{VT}$ at 4-6 GeV/c.

(iv) Some idea of the discrepancies between the different data sets, both old and new, can be obtained from fig. 3. We note that:

(i) At large $|t|$, preliminary FNAL $\pi^+ p \rightarrow K^+ \Sigma^+$ data from ref. 9 lie above the simplest Regge pole extrapolations from lower energies as exemplified by the NS model curves superimposed. Classical absorption models predict this (see below).

(ii) At large $|t|$, preliminary FNAL $\pi^+ p \rightarrow K^+ \Sigma^+$ data from ref. 9 lie above the simplest Regge pole extrapolations from lower energies as exemplified by the NS model curves superimposed. Classical absorption models predict this (see below).

(iii) At large $|t|$, preliminary FNAL $\pi^+ p \rightarrow K^+ \Sigma^+$ data from ref. 9 lie above the simplest Regge pole extrapolations from lower energies as exemplified by the NS model curves superimposed. Classical absorption models predict this (see below).

(iv) At large $|t|$, preliminary FNAL $\pi^+ p \rightarrow K^+ \Sigma^+$ data from ref. 9 lie above the simplest Regge pole extrapolations from lower energies as exemplified by the NS model curves superimposed. Classical absorption models predict this (see below).

(v) At large $|t|$, preliminary FNAL $\pi^+ p \rightarrow K^+ \Sigma^+$ data from ref. 9 lie above the simplest Regge pole extrapolations from lower energies as exemplified by the NS model curves superimposed. Classical absorption models predict this (see below).

(vi) At large $|t|$, preliminary FNAL $\pi^+ p \rightarrow K^+ \Sigma^+$ data from ref. 9 lie above the simplest Regge pole extrapolations from lower energies as exemplified by the NS model curves superimposed. Classical absorption models predict this (see below).

(vii) At large $|t|$, preliminary FNAL $\pi^+ p \rightarrow K^+ \Sigma^+$ data from ref. 9 lie above the simplest Regge pole extrapolations from lower energies as exemplified by the NS model curves superimposed. Classical absorption models predict this (see below).

(viii) At large $|t|$, preliminary FNAL $\pi^+ p \rightarrow K^+ \Sigma^+$ data from ref. 9 lie above the simplest Regge pole extrapolations from lower energies as exemplified by the NS model curves superimposed. Classical absorption models predict this (see below).

(ix) At large $|t|$, preliminary FNAL $\pi^+ p \rightarrow K^+ \Sigma^+$ data from ref. 9 lie above the simplest Regge pole extrapolations from lower energies as exemplified by the NS model curves superimposed. Classical absorption models predict this (see below).

(x) At large $|t|$, preliminary FNAL $\pi^+ p \rightarrow K^+ \Sigma^+$ data from ref. 9 lie above the simplest Regge pole extrapolations from lower energies as exemplified by the NS model curves superimposed. Classical absorption models predict this (see below).

(xi) At large $|t|$, preliminary FNAL $\pi^+ p \rightarrow K^+ \Sigma^+$ data from ref. 9 lie above the simplest Regge pole extrapolations from lower energies as exemplified by the NS model curves superimposed. Classical absorption models predict this (see below).

(xii) At large $|t|$, preliminary FNAL $\pi^+ p \rightarrow K^+ \Sigma^+$ data from ref. 9 lie above the simplest Regge pole extrapolations from lower energies as exemplified by the NS model curves superimposed. Classical absorption models predict this (see below).

(xiii) At large $|t|$, preliminary FNAL $\pi^+ p \rightarrow K^+ \Sigma^+$ data from ref. 9 lie above the simplest Regge pole extrapolations from lower energies as exemplified by the NS model curves superimposed. Classical absorption models predict this (see below).

(xiv) At large $|t|$, preliminary FNAL $\pi^+ p \rightarrow K^+ \Sigma^+$ data from ref. 9 lie above the simplest Regge pole extrapolations from lower energies as exemplified by the NS model curves superimposed. Classical absorption models predict this (see below).

(xv) At large $|t|$, preliminary FNAL $\pi^+ p \rightarrow K^+ \Sigma^+$ data from ref. 9 lie above the simplest Regge pole extrapolations from lower energies as exemplified by the NS model curves superimposed. Classical absorption models predict this (see below).

(xvi) At large $|t|$, preliminary FNAL $\pi^+ p \rightarrow K^+ \Sigma^+$ data from ref. 9 lie above the simplest Regge pole extrapolations from lower energies as exemplified by the NS model curves superimposed. Classical absorption models predict this (see below).

(xvii) At large $|t|$, preliminary FNAL $\pi^+ p \rightarrow K^+ \Sigma^+$ data from ref. 9 lie above the simplest Regge pole extrapolations from lower energies as exemplified by the NS model curves superimposed. Classical absorption models predict this (see below).

(xviii) At large $|t|$, preliminary FNAL $\pi^+ p \rightarrow K^+ \Sigma^+$ data from ref. 9 lie above the simplest Regge pole extrapolations from lower energies as exemplified by the NS model curves superimposed. Classical absorption models predict this (see below).

(xix) At large $|t|$, preliminary FNAL $\pi^+ p \rightarrow K^+ \Sigma^+$ data from ref. 9 lie above the simplest Regge pole extrapolations from lower energies as exemplified by the NS model curves superimposed. Classical absorption models predict this (see below).

(xx) At large $|t|$, preliminary FNAL $\pi^+ p \rightarrow K^+ \Sigma^+$ data from ref. 9 lie above the simplest Regge pole extrapolations from lower energies as exemplified by the NS model curves superimposed. Classical absorption models predict this (see below).

(xxi) At large $|t|$, preliminary FNAL $\pi^+ p \rightarrow K^+ \Sigma^+$ data from ref. 9 lie above the simplest Regge pole extrapolations from lower energies as exemplified by the NS model curves superimposed. Classical absorption models predict this (see below).

(xxii) At large $|t|$, preliminary FNAL $\pi^+ p \rightarrow K^+ \Sigma^+$ data from ref. 9 lie above the simplest Regge pole extrapolations from lower energies as exemplified by the NS model curves superimposed. Classical absorption models predict this (see below).

(xxiii) At large $|t|$, preliminary FNAL $\pi^+ p \rightarrow K^+ \Sigma^+$ data from ref. 9 lie above the simplest Regge pole extrapolations from lower energies as exemplified by the NS model curves superimposed. Classical absorption models predict this (see below).

(xxiv) At large $|t|$, preliminary FNAL $\pi^+ p \rightarrow K^+ \Sigma^+$ data from ref. 9 lie above the simplest Regge pole extrapolations from lower energies as exemplified by the NS model curves superimposed. Classical absorption models predict this (see below).

(xxv) At large $|t|$, preliminary FNAL $\pi^+ p \rightarrow K^+ \Sigma^+$ data from ref. 9 lie above the simplest Regge pole extrapolations from lower energies as exemplified by the NS model curves superimposed. Classical absorption models predict this (see below).

(xxvi) At large $|t|$, preliminary FNAL $\pi^+ p \rightarrow K^+ \Sigma^+$ data from ref. 9 lie above the simplest Regge pole extrapolations from lower energies as exemplified by the NS model curves superimposed. Classical absorption models predict this (see below).

(xxvii) At large $|t|$, preliminary FNAL $\pi^+ p \rightarrow K^+ \Sigma^+$ data from ref. 9 lie above the simplest Regge pole extrapolations from lower energies as exemplified by the NS model curves superimposed. Classical absorption models predict this (see below).

(xxviii) At large $|t|$, preliminary FNAL $\pi^+ p \rightarrow K^+ \Sigma^+$ data from ref. 9 lie above the simplest Regge pole extrapolations from lower energies as exemplified by the NS model curves superimposed. Classical absorption models predict this (see below).

(xxix) At large $|t|$, preliminary FNAL $\pi^+ p \rightarrow K^+ \Sigma^+$ data from ref. 9 lie above the simplest Regge pole extrapolations from lower energies as exemplified by the NS model curves superimposed. Classical absorption models predict this (see below).

(xxx) At large $|t|$, preliminary FNAL $\pi^+ p \rightarrow K^+ \Sigma^+$ data from ref. 9 lie above the simplest Regge pole extrapolations from lower energies as exemplified by the NS model curves superimposed. Classical absorption models predict this (see below).

(xxxi) At large $|t|$, preliminary FNAL $\pi^+ p \rightarrow K^+ \Sigma^+$ data from ref. 9 lie above the simplest Regge pole extrapolations from lower energies as exemplified by the NS model curves superimposed. Classical absorption models predict this (see below).

(xxxii) At large $|t|$, preliminary FNAL $\pi^+ p \rightarrow K^+ \Sigma^+$ data from ref. 9 lie above the simplest Regge pole extrapolations from lower energies as exemplified by the NS model curves superimposed. Classical absorption models predict this (see below).

(xxxiii) At large $|t|$, preliminary FNAL $\pi^+ p \rightarrow K^+ \Sigma^+$ data from ref. 9 lie above the simplest Regge pole extrapolations from lower energies as exemplified by the NS model curves superimposed. Classical absorption models predict this (see below).

(xxxiv) At large $|t|$, preliminary FNAL $\pi^+ p \rightarrow K^+ \Sigma^+$ data from ref. 9 lie above the simplest Regge pole extrapolations from lower energies as exemplified by the NS model curves superimposed. Classical absorption models predict this (see below).

(xxxv) At large $|t|$, preliminary FNAL $\pi^+ p \rightarrow K^+ \Sigma^+$ data from ref. 9 lie above the simplest Regge pole extrapolations from lower energies as exemplified by the NS model curves superimposed. Classical absorption models predict this (see below).

(xxxvi) At large $|t|$, preliminary FNAL $\pi^+ p \rightarrow K^+ \Sigma^+$ data from ref. 9 lie above the simplest Regge pole extrapolations from lower energies as exemplified by the NS model curves superimposed. Classical absorption models predict this (see below).

(xxxvii) At large $|t|$, preliminary FNAL $\pi^+ p \rightarrow K^+ \Sigma^+$ data from ref. 9 lie above the simplest Regge pole extrapolations from lower energies as exemplified by the NS model curves superimposed. Classical absorption models predict this (see below).

(xxxviii) At large $|t|$, preliminary FNAL $\pi^+ p \rightarrow K^+ \Sigma^+$ data from ref. 9 lie above the simplest Regge pole extrapolations from lower energies as exemplified by the NS model curves superimposed. Classical absorption models predict this (see below).

(xxxix) At large $|t|$, preliminary FNAL $\pi^+ p \rightarrow K^+ \Sigma^+$ data from ref. 9 lie above the simplest Regge pole extrapolations from lower energies as exemplified by the NS model curves superimposed. Classical absorption models predict this (see below).

(xl) At large $|t|$, preliminary FNAL $\pi^+ p \rightarrow K^+ \Sigma^+$ data from ref. 9 lie above the simplest Regge pole extrapolations from lower energies as exemplified by the NS model curves superimposed. Classical absorption models predict this (see below).

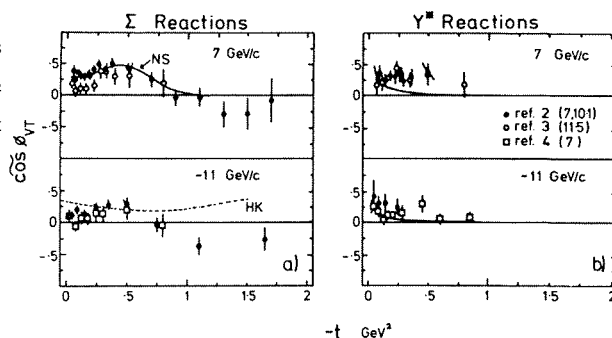
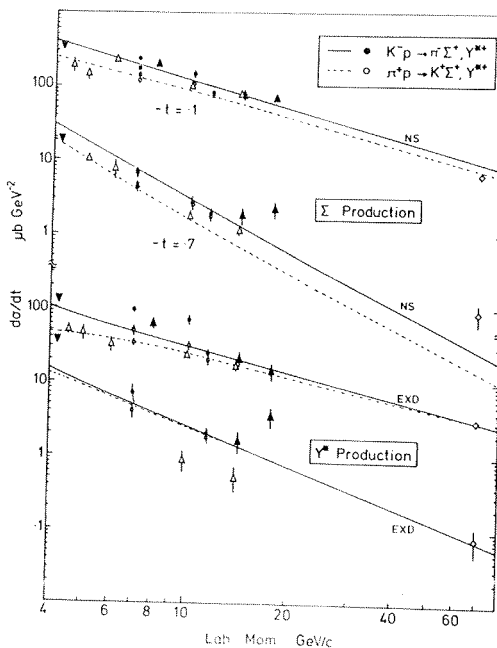


Fig. 2 $\tilde{\cos}\phi_{VT}$ for the Σ and Y^* data of refs. 2,3 and 4. The Σ data of ref. 2 are actually at fixed t' rather than t . This makes little difference.

Some idea of the discrepancies between the different data sets, both old and new, can be obtained from fig. 3. We note that:

(i) At large $|t|$, preliminary FNAL $\pi^+ p \rightarrow K^+ \Sigma^+$ data from ref. 9 lie above the simplest Regge pole extrapolations from lower energies as exemplified by the NS model curves superimposed. Classical absorption models predict this (see below).

Fig. 3 $d\sigma/dt$ at fixed $|t|$ (.1 and .7) for processes (1) and (2). The recent data of refs. 2, 4 and 9 are distinguished by the symbols \circ , \square and \diamond respectively.



(ii) The curves through the Y^* data correspond exactly to those of fig. 2b, i.e. weak EXD + kinematics). The basic pole dependence ($\bar{\alpha}(t = -.1 = .43$, $\bar{\alpha}(t = -.7 = .08$) has been chosen arbitrarily just to guide the eye. The kinematic effect is small compared to discrepancies between data sets.

The result of fits, $\sigma \propto s^{2\alpha_{\text{eff}}(t)-2}$, to the π^+p data is summarised in the α_{eff} plots of fig. 4.

(i) Below 10 GeV/c and for $|t| \lesssim 1$, α_{eff} for $\pi^+p \rightarrow K^+\Sigma^+$ is much above the expected trajectory $\alpha_{K^*} \approx .35 + .9t$, presumably due to the destructive effects of low-lying cuts.⁵⁾ That of $K^-p \rightarrow \pi^-\Sigma^+$ (not shown) is closer to expectation.²⁾

(ii) Over the higher momentum range (10-70 GeV/c) α_{eff} at small t is nearer the leading pole trajectory but deviates at larger t . It is reminiscent of the classical absorption model expectation, exemplified in the figure by the prediction of Hartley and Kane⁶⁾ for this range (dotted curve).

The structure in α_{eff} at $t = -.5$ corresponds to the fact that $d\sigma/dt$ still has a shoulder at $|t| \gtrsim .5$ at 70 GeV/c. Pure Regge pole models tend to have a smooth (exponential) $d\sigma/dt$ in these particular processes (1,2). The structure seen at FNAL⁹⁾ is good evidence for cut effects. The K^-p data at FNAL energies is not yet available.

(iii) Normalisation discrepancies prevent any firm conclusions about the Y^* data.

Overall we see that the evidence is very much against weak EXD even for the helicity flip dominated processes. Approximate agreement between σ_R and σ_C at one momentum (~ 11 GeV/c)³⁾ is not sufficient evidence for EXD. A model with approximately EXD K^* , K^{**} poles supplemented by low-lying cuts⁵⁾ fits the intermediate energy data very well. However, traditional high-lying absorptive cuts must also be present since the polarisation in $\pi^+p \rightarrow K^+\Sigma^+$ remains quite large ($\sim 50\%$) at 70 GeV/c⁹⁾ and since the α_{eff} at large t rises over the higher energy range. Existing models (e.g. ref. 5,6, 7,10) are insufficiently complicated to reproduce these features.

4. Y^* PRODUCTION AMPLITUDES

The weak hyperon decay allows one to reconstruct the spin amplitudes of each Y^* process (2) up to 2 undetermined pieces of information, one of which is the overall phase. If transversity spin quantisation is used, one can

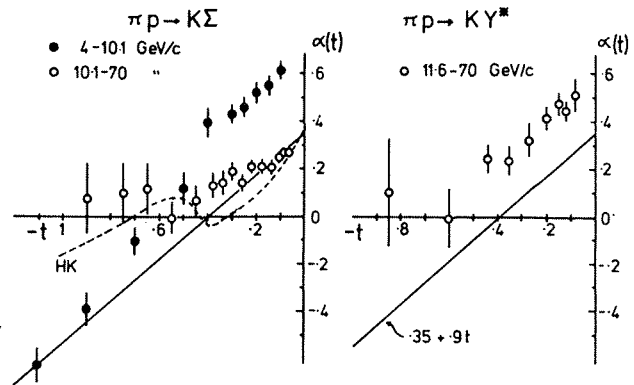


Fig. 4 $\alpha_{\text{eff}}(t)$ evaluated over the momentum ranges shown. The 4-10.1 GeV/c data are from ref. 2. The Y^* data used were those of ref. 3,9. Using the data of ref. 2 instead of ref. 3, α_{eff} is changed by $\Delta \alpha \approx -.07$.

express the results as 4 amplitude moduli (fig. 5) and 2 relative phases. The 11.5 GeV/c data for $K^-p \rightarrow \pi Y^*$ (11) are very similar to those at 4.2 GeV/c. (12) All data agree with the naive quark model expectation (dotted line on fig. 5) that

$$|T_{m_{Y^*} m_P}| = \begin{cases} 0 \\ \frac{1}{\sqrt{2}} \end{cases} \text{ acc. as } |m_{Y^*} - m_P| = \begin{cases} 2 \\ 0 \end{cases} \quad (12)$$

except at small $|t'|$. These deviations are not so surprising since the cross-section already shows a finite helicity non-flip component (zero if equation 12 holds) at $t' \approx 0$. Transversity double-flip can only arise in the quark model via double scattering and so the deviations from (12)

should drop with energy. Apart from $|T_{-3/2 \ 1/2}|$, the data are consistent with this. The preliminary data at 7 GeV/c, however,

show the opposite trend, if any. One must await the final data.

Looking at the differences between KY^* and πY^* amplitudes, one notices that the deviations from the quark model follow different patterns. However, one notices, quite empirically, that the 7 and 11.5 GeV/c data satisfy

$$|T_{m' m}(KY^*)| \approx |T_{m' -m}(\pi Y^*)| \quad (13)$$

in this normalisation, although I know of no theoretical justification for this.

5. OUTLOOK

Basic Regge ideas still represent our only global understanding of the huge mass of long-range hadronic interactions. Hypercharge exchange reactions (1) and (2) provide a particularly severe test of these ideas. The latest data, while confirming these at a qualitative level, also underline the depth of our ignorance when it comes to the details. Believers in QCD will not see this as a significant problem - one simply has to demonstrate confinement, check a few simple perturbative predictions of short distance phenomena and leave the rest to the chemists.

In conclusion, the data from this latest (and probably the last) generation of two-body hadronic experiments is of very high quality indeed and provides many answers. It is unfortunate that few can remember what

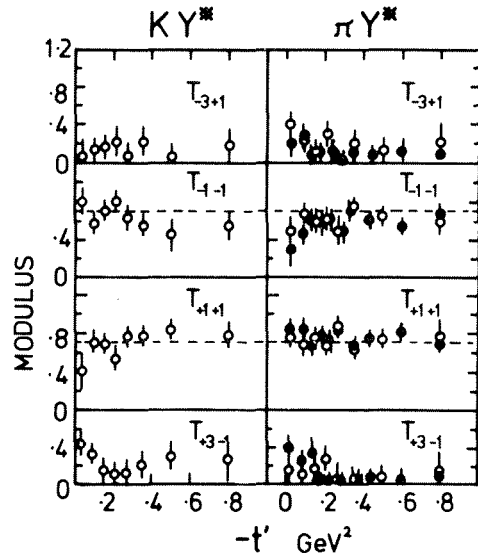


Fig. 5 Transversity amplitude moduli of reactions (2) at 11.5 GeV/c (O) (11) and at 4.2 GeV/c for $K^-p \rightarrow \pi Y^*$ (●) (12). The amplitudes are normalised to unity.

the questions were.

Acknowledgements

I thank T.S. Virdee for communicating experimental results prior to publication and H. Navelet for providing model calculations. I am also grateful to CERN Theory Division for support during preparation of this report.

* * *

References

- 1) A.C. Irving and R.P. Worden, Phys. Reports 34C, 117 (1977), and references therein.
- 2) A. Berglund et al., Phys. Letters 57B, 100 (1975); *ibid.* 73B, 369 (1978). Nucl. Phys. B (to be published).
A. Berglund, Univ. of Stockholm Thesis (1978).
- 3) J. Ballam et al., Phys. Rev. Letters 41, 676 (1978), and private communication from V. Cautis (1979).
- 4) P.A. Baker et al., preliminary data in Imperial College preprint IC/HEMP/78/21 submitted to the XIX int. conf. on high energy physics, Tokyo, Japan (1978); finalised data to be submitted to Nucl. Phys. B (private communication from T.S. Virdee).
- 5) H. Navelet and P.R. Stevens, Nucl. Phys. B104, 171 (1976).
- 6) B.J. Hartley and G.L. Kane, Nucl. Phys. B57, 175 (1973).
- 7) G. Girardi, J. Phys. G3, 1031 (1977).
- 8) G. Girardi et al., Nucl. Phys. B69, 107 (1974).
- 9) M.W. Arenton et al., Argonne report ANL-HEP-RP-78-24.
- 10) G.L. Kane and A. Seidl, Rev. Mod. Phys. 48(2), 309 (1976).
- 11) C.V. Cautis et al., SLAC-PUB-2233 (1978), submitted to Nucl. Phys. B.
J. Ballam et al., IC/HEMP/78/22 submitted to the XIX int. conf. on high energy physics, Tokyo, Japan (1978).
- 12) S.O. Holmgren et al., Nucl. Phys. B119, 261 (1977).